Integrative Modeling of Wireless RF Links for Train-to-Wayside Communication in Railway Tunnel

Shi Pu* and Jian-Hong Hao

Abstract In railway tunnel environment, the reliability of a high-data-rate and real-time train-to-wayside communication should be maintained especially when high-speed train moves along the track. In China and Europe, the communication frequency around 900 MHz is widely used for railway applications. At this carrier frequency band, both of the solutions based on continuously laid leaky coaxial cable (LCX) and discretely installed base-station antennas (BSAs), are applied in tunnel radio coverage. Many available works have concentrated on the radio-wave propagation in tunnels by different kinds of prediction models. Most of them solve this problem as natural propagation in a relatively large hollow waveguide, by neglecting the transmitting/receiving (Tx/Rx) components. However, within such confined areas like railway tunnels especially loaded with train, the complex communication environment becomes an important factor that would affect the quality of the signal transmission. This paper will apply a full-wave numerical method to this case, for considering the BSA or LCX, train antennas and their interacted environments, such as the locomotive body, overhead line for power supply, locomotive pantograph, steel rails, ballastless track, tunnel walls, etc.. Involving finite-difference time-domain (FDTD) method and uni-axial anisotropic perfectly matched layer (UPML) technique, the entire wireless RF downlinks of BSA and LCX to tunnel space to train antenna are precisely modeled (so-called integrative modeling technique, IMT). When exciting the BSA and LCX separately, the field distributions of some cross-sections in a rectangular tunnel are presented. It can be found that the influence of the locomotive body and other tunnel environments is very significant. The field coverage on the locomotive roof plane where the train antennas mounted, seems more homogenous when the side-laying position of the BSA or LCX is much higher. Also, much smoother field coverage solution is achieved by choosing LCX for its characteristic of more homogenous electromagnetic wave radiation.

Key Words : Train Antenna, Leaky Coaxial Cable, Base-Station Antenna, Rectangular Tunnel, Integrative Modeling Technique.

1. Introduction

Reliability of high-data-rate and real-time train-to-wayside communication must be maintained when high-speed train moves along the railway track. Hence, it is vital to study the wireless RF link precisely and to know the properties of the link clearly. Commonly, solutions based on continuously laid leaky coaxial cable (LCX) would provide much smoother signal coverage for their characteristics of homogenous electromagnetic wave radiation and no blind spot, than those based on discretely installed base-station antennas (BSAs). However, when using LCX, there still exists some disadvantages,

* Institute of Modern Electronic Technology, School of Electricaland Electronic Engineering

such as high cost of installation and maintenance, etc., which could be easily avoided by applying BSAs. As the extensive application of wireless communication techniques in China railway, especially in case of railway tunnels for mountain areas, it is very important and valuable to acquire the capability of designing environmentally suitable BSAs and LCXs, determining optimum side-laying positions, and estimating the coverage, without making massive measurements on-site, which are very expensive and time-consuming. Thereby, in order to provide some guidelines for this case, it is necessary to develop efficient methods for accurately modeling of the wireless RF link. Two types of the wireless RF link based on LCX or BSAs are both discussed in this paper. Taking the downlink for example, the entire wireless RF link described here would be divided into the following three parts [1], [2]: the radiating of RF signal by LCX or BSA, the propagating of the signal wave in tunnel loaded with train body and its environment, and the receiving of the RF signal by train antenna.

Many available works have concentrated on the radio-wave propagation in tunnels by different kinds of prediction models. The majority of them concern about the second part of the entire wireless RF link as mentioned above, without considering the effects of the transmitting/receiving (Tx/Rx) components and their interactions with surrounding environments [3], or just about the natural propagation like in a relatively large hollow waveguide [4]. Also, some literatures about radio coverage prediction of BSAs and LCX for tunnel or indoor scenarios have been reported [5]-[10]. The core idea is to assume the BSA or LCX to be an equivalent source or source array first, and then to estimate the wireless coverage by ray-tracing method. The prediction of them could be very successful in the case of relatively empty tunnel, indoor scenarios, or with simply periodic structures, where the RF signals radiating from the BSA or LCX in its far-field area can be treated as local plane waves, so that the ray-tracing method is valid based on this assumption. But within the complex confined areas like railway tunnels especially loaded with the train body, the communication environment becomes a very important factor that would affect the quality of the RF signal transmission. The ray-based solutions are not sufficiently accurate in the regions close to complex discontinuities. Thus the complex communication environment should not be neglected or roughly approximated. To this end, in this paper, a full-wave numerical method will be applied for considering not only the propagation mechanisms of multi-path reflecting, scattering, diffracting, etc., but also the effects of Tx/Rx components.

By involving finite-difference time-domain (FDTD) method with uni-axial anisotropic perfectly matched layer (UPML) technique, the entire wireless RF link of LCX or BSA to tunnel space to train antenna will be precisely modeled. Here, the BSA or LCX, train antennas and their interacted environments, such as the locomotive body, overhead line for power supply, locomotive pantograph, steel rails, ballastless track, tunnel walls, etc., can be all taken into account. In China and Europe, the carrier frequencies around 900 MHz are widely used for modern railway wireless communications. Firstly, at the operating frequency of 900 MHz, the influences of different installation positions of BSA or LCX on the output signal of the monopole antenna mounted upon the locomotive roof (so-called locomotive antenna) are analyzed here in this paper. Then some numerical results including the field distributions on cross-sections of a rectangular tunnel with variable installation locations of BSA or LCX will be presented.

2. Theory and method

In this paper, the wireless RF downlink defined is starting from the input terminal of the BSA or LCX to the output terminal of the locomotive antenna (Rx), while the uplink defined is starting from the input terminal of the locomotive antenna (Tx) to the output terminal of the BSA or LCX. Both links compose the train-to-wayside communication in railway tunnel, as shown schematically in Figure 1. Figure 1(a) depicts the configuration implemented using the BSAs inside tunnel and outside. Different from this case, Figure 1(b) describes the configuration realized by the LCX in tunnel and the BSAs outside. In the second case, there is one BSA at the entrance with the LCX connected to it and another BSA at the exit of the tunnel. The high-speed train is running towards $-y$-direction with velocity of v and real-timely communicating with discretely installed BSA or continuously laid LCX along y-direction in the rectangular railway tunnel. At the operating frequency band of 900 MHz, four Tx/Rx antennas are mounted upon the train locomotive (locomotive antennas) for different use. Under the illuminating of the BSAs or LCX in tunnel, the ideal coverage of these two cases can be seen in Figure 1.

For precisely modeling of the entire wireless RF link, the FDTD method of the Yee's mesh grid combined with the UPML technique as in [1] are applied here to study the area including one BSA or LCX, four locomotive antennas and the surrounding railway environment interacted with them, thus called *integrative modeling technique* (*IMT*).

By considering the limitations of computer memory and running time, the artificial rectangular box surface drawn in Figure 1, which includes the entire wireless RF link in the railway tunnel, is restricted to the UPML inner surface in FDTD computation domain, as illustrated in Figure 2. So in the integrative computation model, only the significant channel environments near the Tx/Rx components are considered, such as the locomotive body of the whole train, overhead line for power supply, locomotive pantograph, steel rails, ballastless track and tunnel walls. In FDTD, these environmental models are discretized into cubic meshes all with the grid size of ΔS = 0.028 m, in

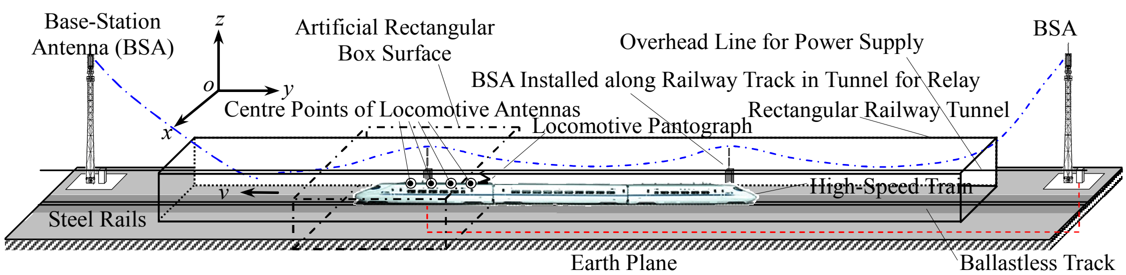

(a) The case based on base-station antennas (BSAs).

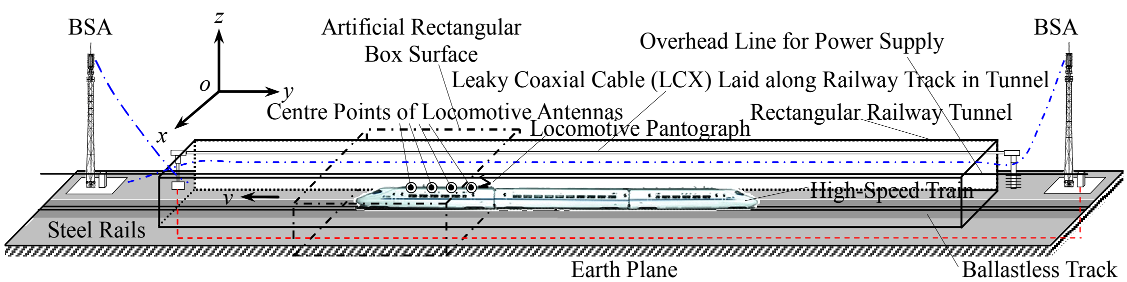

(b) The case based on leaky coaxial cable (LCX).

Figure 1. Schematic diagram of wireless RF link for train-to-wayside communication in tunnel.

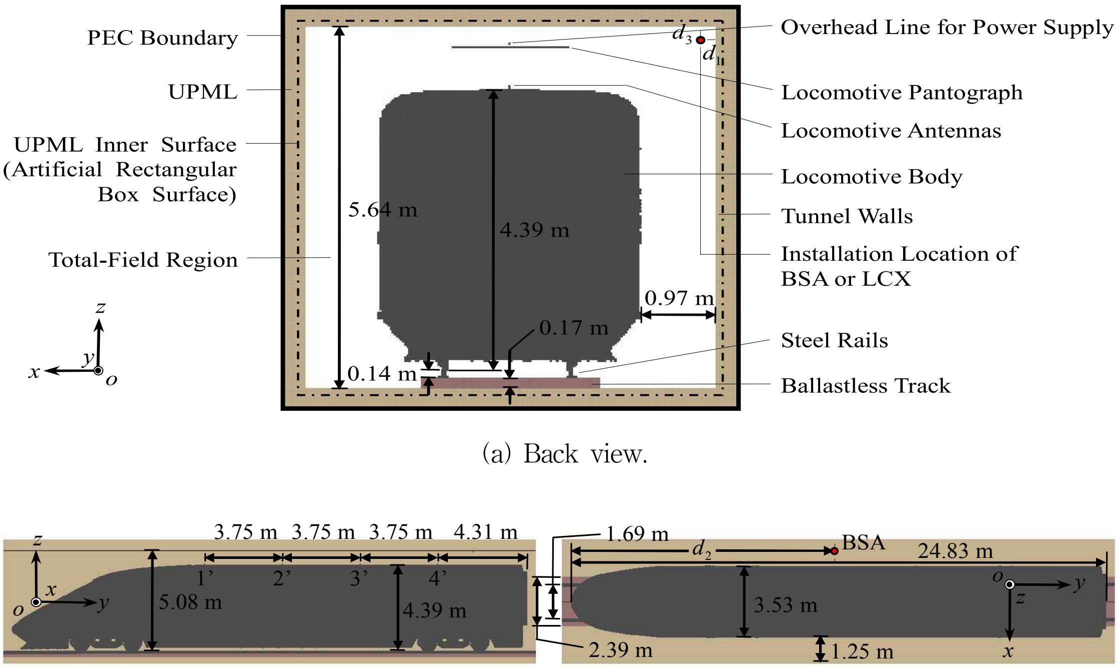

(a) Back view.

(b) Side view. (c) Top view.

Figure 2. Cross-sections of integrative computation model of wireless RF link in tunnel.

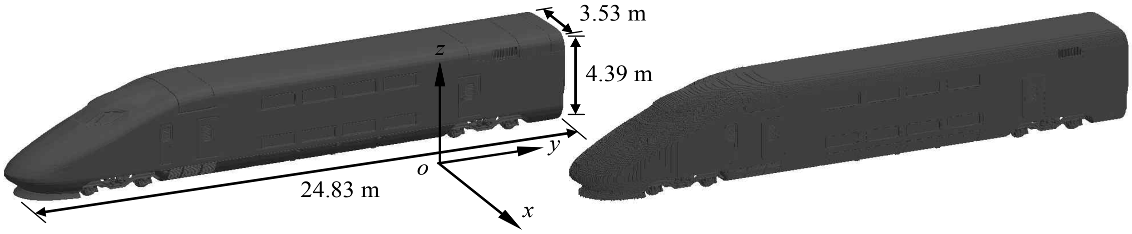

(a) Original object model. (b) Uniformly meshed model.

Figure 3. Three-dimensional geometric model of train locomotive body.

<Table 1> List of electromagnetic parameters of materials

Object	Material	ε_r (-)	μ_r (-)	σ (S/m)
Locomotive Body	Aluminum Alloy	1.0	1.0	2.494×10^{7}
Overhead Line for Power Supply	Copper	1.0	1.0	5.8×10^{7}
Locomotive Pantograph	Dip Metal Carbon Slide Plate	1.0	1.0	2.5×10^{5}
Steel Rails	Stainless Steel	1.0	1.0	1.1×10^{6}
Ballastless Track	Concrete	6.0	1.0	1.95×10^{-3}
Tunnel Walls	Concrete	6.8	1.0	3.4×10^{-2}

which the original object model and uniformly meshed model of the train locomotive body are depicted in Figure 3. The locomotive body has the maximum size of 3.53 m × 24.83 m × 4.39 m (corresponding to 127👎S, 894👎S, 158👎S in x-, y-, z-direction respectively), and is running in the middle of the 5.5-m-wide straight rectangular-shaped single-track railway tunnel with height of 5.64 m. Locating 0.72 m ($26\Delta S$) above the centre of the locomotive roof in *y*-direction, the overhead line for power supply has the cross-section size of $1\Delta S \times 1\Delta S$. Below and crossing with the overhead line for power supply, the 1.56-m-long pantograph also has the cross-section size of $1\Delta S \times 1\Delta S$. The other size parameters are given in Figure 2. In terms of infinity approximation to the actual situation, the objects like the overhead line for power supply, steel rails, ballastless track and tunnel walls are extended into the UPML in the *IMT*. The electromagnetic material parameters of these object models are listed in Table 1, where ε_r, μ_r and σ denote the relative permittivity, relative permeability and electric conductivity respectively.

Here in this paper, the operating frequency for the train-to-wayside communication systems is set to 900 MHz. There are totally four quarter-wavelength monopole antennas mounted upon the locomotive along the central line in *y*-direction. The monopole model of the locomotive antennas used here is composed of the monopole arm part by using thin-wire approximation and the coaxial line part by taking TEM-mode iteration, which is the same as in [2]. In the coverage configuration as shown in Figure 1(a), the BSA installed in tunnel for relay is a half-wavelength dipole antenna. It is simulated by gap feed model with the gap size of $1\Delta S$ between two dipole arms. But in the coverage configuration as seen in Figure 1(b), a radiating-mode inclined slot LCX is chosen instead of the BSAs. On the outer conductor of the LCX, there are two dual inclined slots carved in each period of P [11]. This kind of the slot array structure could suppress the even-order and −3-order spatial harmonics, thus the radiation frequency band of single-mode harmonic is expanded. By equivalent principle and image theorem, the radiating LCX is approximated as an array of magnetic dipoles, and then it can be integrated into the computation domain of the IMT.

3. Numerical results and discussion

Both of the wireless RF links based on the BSA and LCX irradiating in railway tunnel are analyzed separately by applying the *IMT* described above. As depicted in Figure 2, the whole computation domain is divided into 218 × 924 × 223 cells, including the outer layer of 8 cells for UPML modeling. The space-step and time-step are set to ΔS = 0.028 m and $\Delta t = \Delta S/(2c)$ = 0.046 ns respectively, where c is the velocity of light. The four locomotive antennas and their feeding coaxial cables are of the same parameters: the radius of inner conductor a = 2.53 mm, the radius of inner surface of outer conductor b = 5.82 mm, and the coaxial dielectric ε_r = 1.0. Here in Figure 2, the 1st, 3rd and 4th locomotive antennas marked as 1', 3' and 4' are taken as the Tx antennas, while the 2nd locomotive antenna marked as 2' is treated as the Rx antenna. With the knowledge of receiving and radiating characteristics of train antennas on locomotive roof as given in [1], the field strength level in the area above the locomotive roof is much higher than that in other areas. Furthermore, the suitable positions where the BSA or LCX is installed, still need to be optimized and determined for acquiring reliable signal transmission.

Usually, the BSA or LCX is hung on one side of the tunnel walls. The distances between the BSA or LCX and the tunnel wall are marked as d_1, d_3 depicted in Figure 2. Under the excitation of the BSA laid at positions of d_1 = 0.194 m, d_3 = 0.194 m, 0.472 m, 0.75 m and 1 m respectively, the field distributions of the tunnel in *xoy*-plane through the locomotive roof plane and centre points of four locomotive antennas, are drawn in Figure 4. The situations under the excitation of the LCX located at the corresponding positions as the BSA, have also been calculated for comparison as shown in

Figure 5 [11]. What's different is that the BSA here is installed at the centre of this tunnel section (corresponding to d_2 = 12.42 m), while the LCX is laid continuously through the tunnel. From Figure 4 and 5, it is seen that the field coverage on the locomotive roof where the locomotive antennas are mounted, seems more homogenous or stronger when the side-laying position of the BSA or LCX is much higher in tunnel space. Obviously, the configuration based on the LCX owns much smoother tunnel coverage than that based on the BSA. Also, the variations of the output voltage of the Rx locomotive antenna 2' with the installation location of the BSA and LCX are presented separately as shown in Figure 6. Assuming that the train leaves out of the tunnel, the field distributions within empty tunnel are recalculated as shown in Figure 7 and 8. From these two figures, we can find that the influence of the locomotive body and other tunnel environment is very significant.

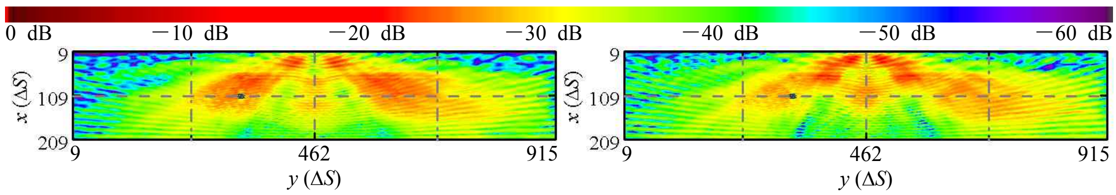

(a) When BSA is laid at $d_3 = 7\Delta S$. (b) When BSA is laid at $d_3 = 17\Delta S$.

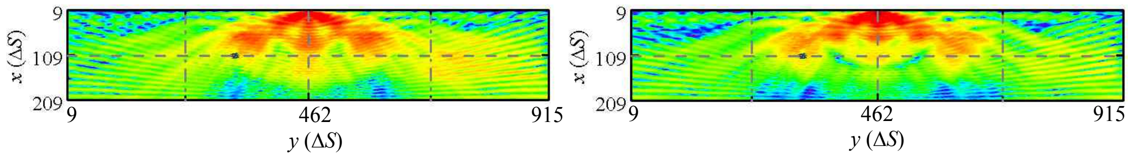

(c) When BSA is laid at $d_3 = 27\Delta S$. (d) When BSA is laid at $d_3 = 36\Delta S$.

Figure 4. Field distributions within railway tunnel for different positions of BSA.

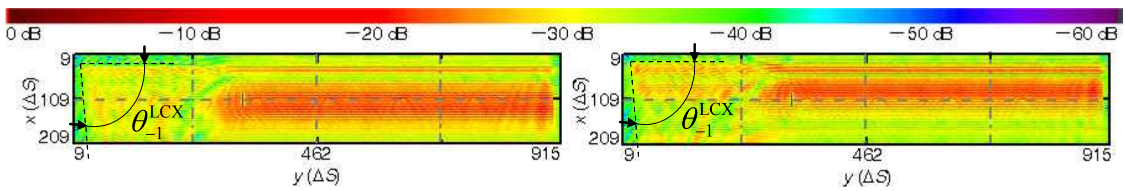

(a) When LCX is laid at $d_3 = 7\Delta S$. (b) When LCX is laid at $d_3 = 17\Delta S$.

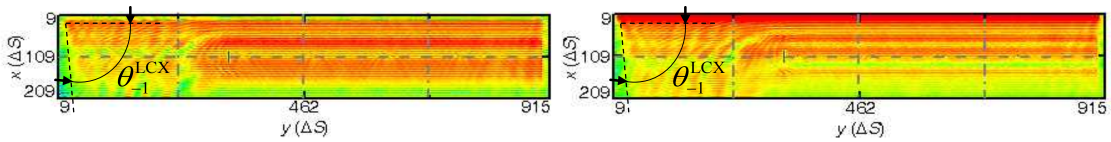

(c) When LCX is laid at $d_3 = 27\Delta S$. (d) When LCX is laid at $d_3 = 36\Delta S$.

Figure 5. Field distributions within railway tunnel for different positions of LCX.

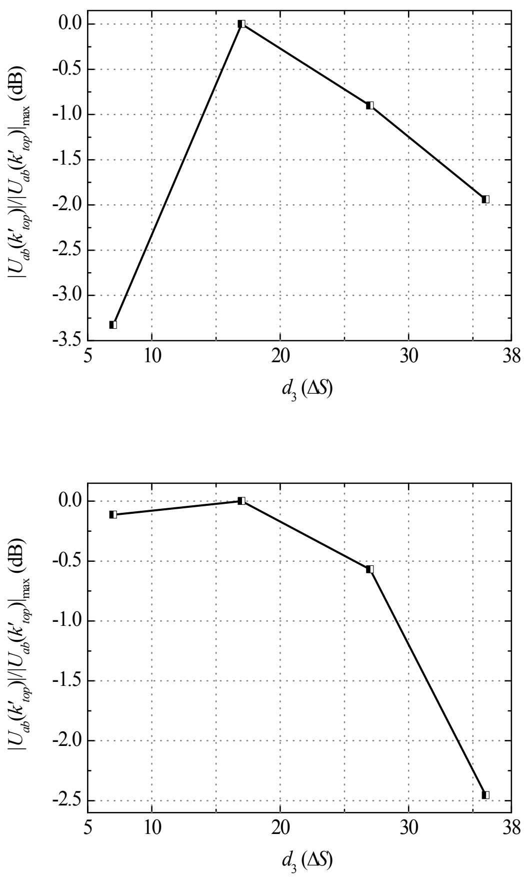

(a) Solution based on BSA. (b) Solution based on LCX.

Figure 6. Variations of output voltage of locomotive antenna 2' with installation location of BSA or LCX.

4. Conclusions

Estimation for the radio coverage inside the railway tunnel is a very important work for the complicated environment of train-to-wayside communication. To include the Tx/Rx components and their surrounding environment, an *IMT* involving the FDTD method and UPML technique is applied in this paper. The entire wireless RF link integratively modeled here (downlink direction) starts from the input of the BSA or LCX and ends up with the output of the locomotive antenna via the tunnel space. At the operating frequency of 900 MHz, the field distributions in a straight rectangular-shaped single-track railway tunnel are calculated under the excitations of the BSA and LCX separately. From these results, we can conclude that the interactions between Tx/Rx components and surrounding environment could not be neglected within such complex confined areas, and better field coverage will be obtained if the BSA or LCX is laid higher on one side tunnel wall. In addition, also by the *IMT*, the variations of the output voltage and current of the locomotive antenna with the illuminating of the BSA and LCX with the train moving, will be studied in the future work.

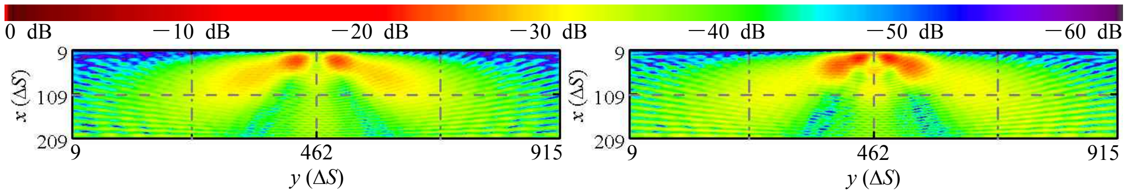

(a) When BSA is laid at $d_3 = 7\Delta S$. (b) When BSA is laid at $d_3 = 17\Delta S$.

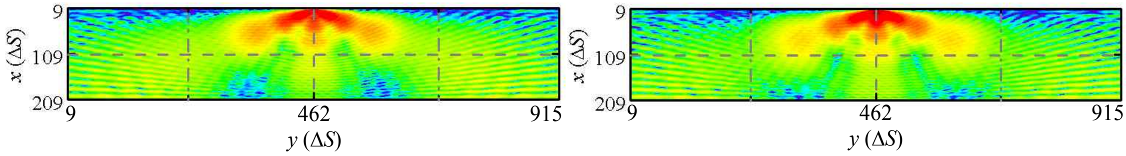

(c) When BSA is laid at $d_3 = 27\Delta S$. (d) When BSA is laid at $d_3 = 36\Delta S$.

Figure 7. Field distributions within railway empty tunnel for different positions of BSA.

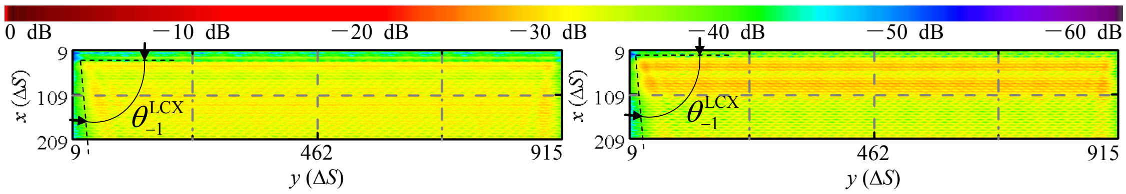

(a) When LCX is laid at $d_3 = 7\Delta S$. (b) When LCX is laid at $d_3 = 17\Delta S$.

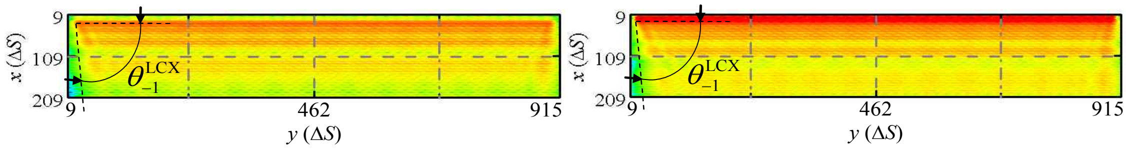

(c) When LCX is laid at $d_3 = 27\Delta S$. (d) When LCX is laid at $d_3 = 36\Delta S$.

Figure 8. Field distributions within railway empty tunnel for different positions of LCX.

References

[1] S. Pu, and J.-H. Wang, "Research on the receiving and radiating characteristics of antennas on high-speed train using integrative modeling technique", The 11th Asia-Pacific Microwave Conference 2009, Singapore, pp. 1072-1075, December 2009.

[2] S. Pu, J.-H. Wang, and Z. Zhang, "Estimation for small-scale fading characteristics of RF wireless link under railway communication environment using integrative modeling technique", *Progress In Electromagnetics Research-PIER*, Vol. 106, pp. 395-417, 2010.

[3] Y. P. Zhang, and Y. Hwang, "Theory of the radio-wave propagation in railway tunnels", *IEEE Transactions on Vehicular Technology*, Vol. 47, No. 3, pp. 1027-1036, 1998.

[4] A. M. Ghuniem, "Modes of electromagnetic wave propagation in circular concrete tunnels", *Journal of Electromagnetic Waves and Applications*, Vol. 19, No. 1, pp. 95-106, 2005.

[5] C. Briso-Rodríguez, J. M. Cruz, and J. I. Alonso, "Measurements and modeling of distributed antenna systems in railway tunnels", *IEEE Transactions on Vehicular*

Technology, Vol. 56, No. 5, pp. 2870-2879, 2007.

[6] R. Hoppe, P. Wertz, F. M. Landstorfer, and G. Wölfle, "Advanced ray-optical wave propagation modelling for urban and indoor scenarios including wideband properties", *European Transactions on Telecommunications*, Vol. 14, No. 1, pp. 61-69, 2003.

[7] F. M. Landstorfer, "Wave propagation models for the planning of mobile communication networks", The 29th European Microwave Conference 1999, Munich, pp. 1-6, 1999.

[8] F. Sayadi, M. Ismail, N. Misran, and K. Jumari, "Radio coverage inside tunnel utilizing leaky coaxial cable base station", *Journal of Applied Sciences*, Vol. 9, No. 16, pp. 2887-2896, 2009.

[9] S. P. Morgan, "Prediction of indoor wireless coverage by leaky coaxial cable using ray tracing", *IEEE Transactions on Vehicular Technology*, Vol. 48, No. 6, pp. 2005-2014, 1999.

[10] H. Cao, and Y. P. Zhang, "Radio propagation along a radiated mode leaky coaxial cable in tunnels", The 4th Asia-Pacific Microwave Conference 1999, Singapore, pp. 270-272, 1999.

[11] S. Pu, J.-H. Wang, and Y.-J. Li, "Calculation of the field distribution in a railway tunnel in presence of train using integrative modelling technique", The 15th International Symposium on Antennas and Propagation 2010, Macau, pp. 535-538, November 2010.

Shi PU

- Wuhan University of Technology (WHUT)
- computer science from Wuhan University (WHU)
- degree in electrical engineering from Beijing Jiaotong University (BJTU)
- Institute of Modern Electronic Technology

Jian-Hong Hao